http://dx.doi.org/10.6493/SmartSci.2015.317

Effect of Particle Size on Shear Stress of Magnetorheological Fluids

Chiranjit Sarkar[1,*] **and Harish Hirani**[2]

[1]Department of Mechanical Engineering, Delhi Technological University, Delhi, India
[2]Department of Mechanical Engineering, Indian Institute of Technology Delhi, New Delhi, India
* Corresponding Author / E-mail: chiranjit.ju@gmail.com, TEL: +91-95-821-83980, FAX: +011-2787-1023

KEYWORDS : Magnetorheological fluids, Particle size distributions, Variable shear stress, Large size particles, Smaller size particles

Magnetorheological fluids (MRF), known for their variable shear stress contain magnetisable micrometer-sized particles (few micrometer to 200 micrometers) in a nonmagnetic carrier liquid. To avoid settling of particles, smaller sized (3-10 micrometers) particles are preferred, while larger sized particles can be used in MR brakes, MR clutches, etc. as mechanical stirring action in those mechanisms does not allow particles to settle down. Ideally larger sized particles provide higher shear stress compared to smaller sized particles. However there is need to explore the effect of particle sizes on the shear stress. In the current paper, a comparison of different particle sizes on MR effect has been presented. Particle size distributions of iron particles were measured using HORIBA Laser Scattering Particle Size Distribution Analyser. The particle size distribution, mean sizes and standard deviations have been presented. The nature of particle shapes has been observed using scanning electron microscopy. To explore the effect of particle sizes, nine MR fluids containing small, large and mixed sized carbonyl iron particles have been synthesized. Three concentrations (9%, 18% and 36% by volume) for each size of particles have been used. The shear stresses of those MRF samples have been measured using ANTON PAAR MCR-102 Rheometer. With increase in volume fraction of iron particles, the MR fluids synthesized using "mixed sized particles" show better shear stress compared to the MR fluids containing "smaller sized spherical shaped particles" and "larger sized flaked shaped particles" at higher shear rate.

Manuscript received: December 23, 2014 / Accepted: January 26, 2015

1. Introduction

Magnetorheological fluids (MRF) are synthesized by suspending magnetisable micrometer -sized particles (few micrometers to 200 micrometers) in a nonmagnetic carrier liquid [1]. The variable shear stress of MRF can be regulated in milliseconds [2-3]. The magnetisable particles, in the presence of magnetic field, acquire dipolar energy to interact among each other and form structure. The structure made by particles provides shear stress (perpendicular to the direction of magnetic field) to the MRF. Shear stress of MRF not only depends on the magnetic field, but also on the volume fraction of the particles and particle sizes. As per Lemaire et al. [4]; Kittipoomwong and Klingenberg [5]; Chiriac and Stoian [6], increasing particle sizes augments shear stress of MRF. However due to sedimentation problem, usage of larger sized particles [7-8] are discouraged. Similarly, retainability of magnetic field in submicron particles [9] is disadvantageous as quick reversibility in shear stress is an essential functionality of MR fluids. It is interesting to note that the cost of larger sized particles is just 28% of the cost of smaller sized particles [10]. From this deliberation, it can be inferred that MR applications incorporating mechanical stirring (such as brakes, clutches) may use larger sized particles. To create complete chaining mechanism of MR fluids, the volume fractions of iron particles should be in between 20% - 40% [11-14]. To explore the effect of particle sizes, nine MR fluids containing 9%, 18% and 36% by volume carbonyl iron (CI) small, large and mixed sized particles have been synthesized. The shear stress with various magnetic fields at constant shear rate has been measured using MCR-102 Rheometer. The results have been presented in the manuscript.

2. Particle size distribution

As per Lemaire et al. [4] small sized particle means diameter = 0.5 μm and large sized particle means diameter = 1.0 μm. As per Kittipoomwong and Klingenberg [5], the larger size means two times the size of smaller size particle. Chiriac and Stoian [6] termed particle lesser than 20μm as smaller sized particle, while particles in the range of 50 to 63 μm were named as larger sized particles. This review of literature intimates the subjective nature of term "larger sized" and "smaller sized" particles. In the present case, two commercial carbonyl iron powders; and product no. 12310 and 44890 from Sigma Aldrich, were purchased. The product no. 12310 contains approximately 10% in the range 150μm - 212μm, 65 - 85% in the range of 45μm - 150μm. Therefore the Product No. 12310 is named as "large sized particles". The particle size distribution in product No.

44890 varies in the range of 3.4 µm to 33.0 µm; and this product No. 44890 is named as "small sized particles". Fig. 1 shows the probability volume density graph of "small sized particle". Fig. 2 shows the probability volume density graph of "large sized particle". The particle size distributions were measured using HORIBA Laser Scattering Particle Size Distribution Analyzer LA-950. Iron particles were dispersed in water and used in the funnel of the Analyzer LA-950. Sonication was done to disperse the particles thoroughly. The form of distribution was set at "auto" mode. Particle size distributions calculations were made on the volume basis. Refractory index of iron and water were kept 3.500 - 3.800i and 1.333 respectively. The mean size and standard deviation of the "small sized particle" distributions are 9.27 µm and 4.63 µm respectively. The mean size and standard deviation of the "large sized particle" distributions are 120.85 µm and 56.05 µm respectively.

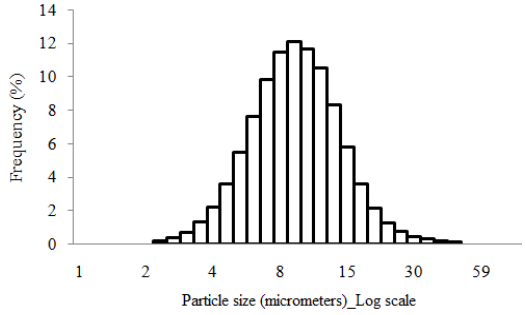

Fig. 1 Probability volume density graph of "small sized particles"

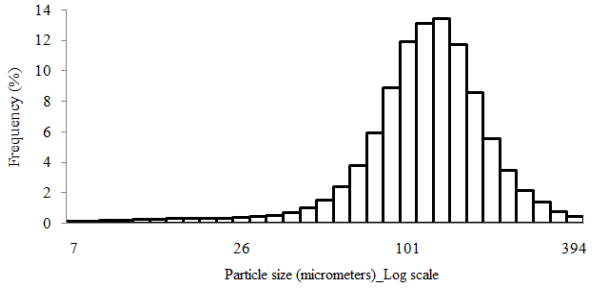

Fig. 2 Probability volume density graph of "large sized particles"

The scanning electron microscope photographs of "small sized particle" and "large sized particle" have been shown in Fig. 3. It shows that the "small sized particles" are spherical in shape and different sizes vary from the 2.269 µm to 44.938 µm. The "larger sized particles" are of flake shape. This flake type iron particle may create more friction and it may rub the rotating disk surfaces. The sizes of larger sized particles vary from 7 µm to 394 µm.

3. Synthesis and characterization of MRF

In this research work, nine MR fluid samples have been prepared. The general nomenclatures of the nine MR fluid samples are MRFXXL, MRFXXS, and MRFXXM1. Where, XX is the volume fraction of iron particles in MR fluid, L is the symbol for larger sized flake shaped particle, S is the symbol for smaller sized spherical shaped particle, M1 is the symbol for 50% of large and 50% of small particles. Here, oleic acid is used as additive and silicone oil is used as carrier fluid. The dynamic viscosity of the carrier fluid is kept as 0.2186 Pa.s at 100 s^{-1} shear rate. The fluid was homogenised in mechanical stirrer. The probability volume density graph of "mixed sized particle" i.e. large (50%) and small (50%) is shown in Fig. 4. The percentage of frequency for "small sized particles" is lower than that for "larger sized particles".

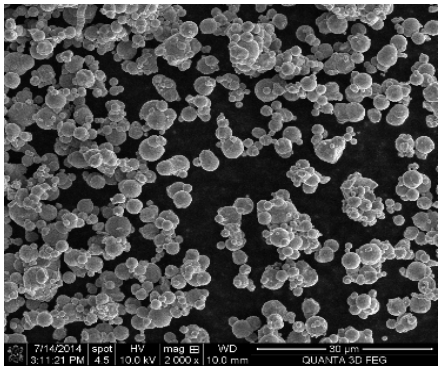

(a) Small sized particles

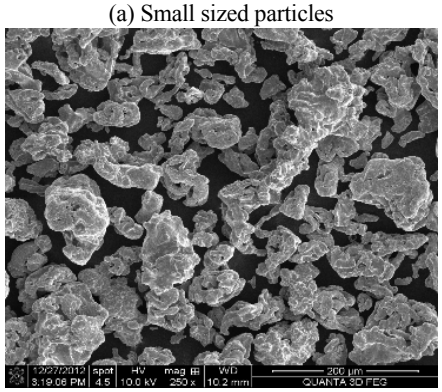

(b) Large size particles

Fig. 3 Scanning Electron Microscopic photographs

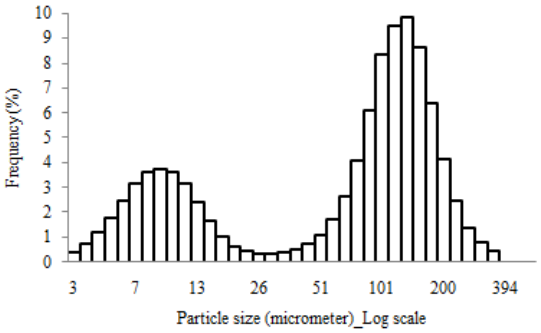

Fig. 4 Probability volume density graph of "mixed sized particle"

Shear stress flow curve of these MR fluid samples have been measured in ANTON PAAR modular compact rheometer MCR-102 at different magnetic fields in controlled shear rate (CSR) mode. The shear rate in the range from 0.1 to 1000 s^{-1} was tested. Shearing MR fluids at higher shear rate expel fluid away from the disks [15-16]. For each shear rate sweep, the measuring point's duration was set from an initial 15s to a final 1s via log-log scale. The measurement was performed in a parallel plate system with a diameter of 20 mm at a gap of 1 mm. The resulting flow responses have been examined as a function of magnetic field strength ranging from 0 to 152.4 kA/m. The magnetic field strength (A/m) has been calculated from the

magnetorheological cell 70/1T MRD. Temperature was set at 30°C during the measurement.

Shear stress of these MR fluid samples have been measured in ANTON PAAR modular compact rheometer MCR-102 at three different shear rates 10 s^{-1}, 100 s^{-1} and 1000 s^{-1}.The measurement was performed in a parallel plate system with a diameter of 20 mm at a gap of 1 mm. The shear stress of MR fluid sample has been measured for various input currents (0.1 to 4.8 A). Magnetic field strength (A/m) has been calculated from the magnetorheological cell 70/1T MRD. Table 1 shows the data of shear stress measurement for MRF09L at10 s^{-1} shear rate. There are 15 measuring points for interval of 10 seconds and shear rate is fixed at constant value. Temperature is set at 29°C during the measurement. The minimum shear stress is 16.69 Pa at 5.316 kA/m magnetic field and 13,700 Pa at 152.40 kA/m magnetic fields.

Table 1 Shear stress measurement of MRF09L at various input currents at 10 s^{-1} shear rate

Current	Meas. Pts.	Time	Shear Rate	Temperature	Magnetic Field Strength	Shear Stress
[A]		[s]	[s^{-1}]	[°C]	[A/m]	[Pa]
0.1	1	10	9.998	28.74	5,316	16.69
0.13	2	20	9.999	28.74	6,743	43.21
0.17	3	30	10	28.74	8,477	72.21
0.23	4	40	9.999	28.74	10,790	112.2
0.3	5	50	10	28.74	14,310	164.9
0.4	6	60	9.995	28.74	18,850	263.7
0.5	7	70	10.01	28.75	24,720	436.8
0.7	8	80	9.993	28.76	32,170	741
0.9	9	90	10	28.77	41,580	1,272
1.2	10	100	10	28.77	53,140	2,143
1.6	11	110	9.985	28.78	67,430	3,486
2.1	12	120	10.01	28.8	84,450	5,472
2.8	13	130	9.961	28.81	1,04,300	8,108
3.6	14	140	10.02	28.84	1,28,400	11,340
4.8	15	150	9.976	28.89	1,52,400	13,700

To understand the shear stress as function of particle size, and magnetic field a number of experiments were conducted and results have been plotted in Fig. 5(a). In the figure, variability of data has been represented by error bar. Fig. 5(a) shows the shear stress of MR fluid (09% volume fraction) at 10 s^{-1} shear rate. The shear stress of all MR fluids increases with increase in magnetic fields, but the effect of magnetic field is more dominated for MRF09L compared to MRF09S and MRF09M1. The difference in behaviour of MRF09L, MRF09S and MRF09M1 can be explained considering flake type large sized particles as observed in the SEM images (as shown in Fig. 3(b)). Hato et al. [16] tested performances of pure CI and CI/15A based MR fluids by conducting experiments in a controlled shear rate mode (CSR) (shear rate ranging from 0.01 to 1000 s^{-1} via a log-log scale) under varying magnetic fields. In line with Hato et al. (2011), to understand the rheological behavior of MR fluids, more experiments have been performed and the shear stress flow curve of all MR fluids samples with a full range of shear rate (0.1 s^{-1} to1000 s^{-1}) have been plotted in a log-log scale.

Fig. 5(b) shows the shear stress flow curve of MR fluids (09% by vol. iron particles) in controlled shear rate mode at 0 kA/m magnetic field. It illustrates larger shear stress of MRF09L compared to that of MRF09S and MRF09M1. For smaller (09%) volume fraction of iron particles, MR fluids with large sized flaked shaped iron particles (L-particles) complete the chain; whereas smaller sized spherical shaped (S-particles) and mixed sized iron particles are unable to make complete chain structure as shown in Fig. 6.

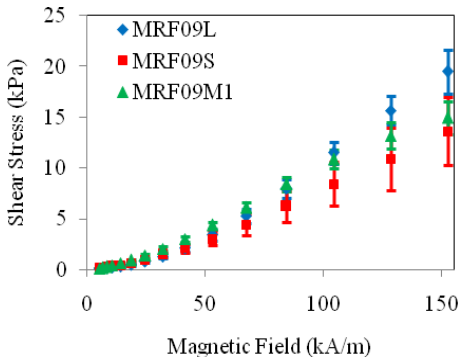

(a)Shear stress of MR fluids at 10 s^{-1} shear rate

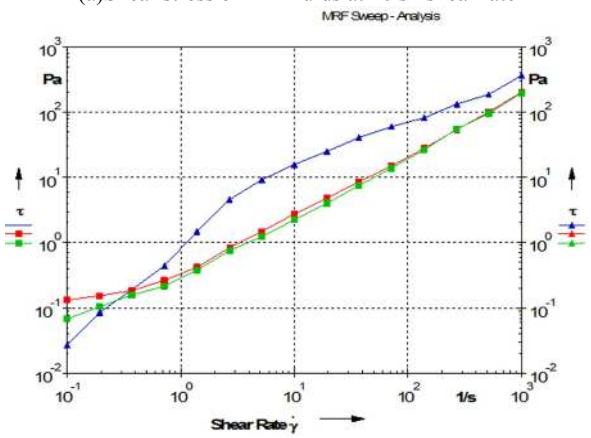

(b) Shear stress flow curve of MR fluids at NO magnetic field

Fig. 5 Shear stress of MR fluid (09 % by vol. iron particles) at 10 s^{-1} shear rate

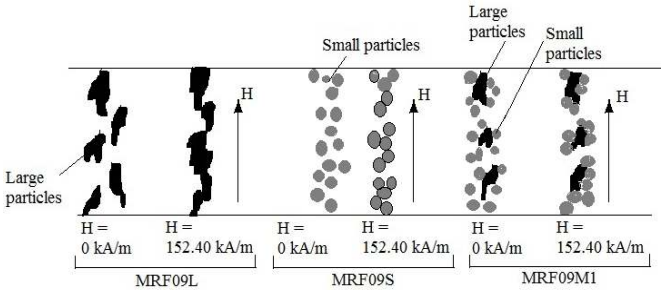

Fig. 6 Chain structure of MR fluids (09% by vol. iron particles)

Fig. 7(a) shows the shear stress of MR fluid (18% volume fraction iron particle) at 10 s^{-1}. The shear stress of MR fluids increases with increase in magnetic fields. Fig. 7(b) shows shear stress flow curve of MR fluids (18% by vol. iron particles). All MR fluids show the increase in shear stress with increase in shear rate at zero magnetic fields. From shear rate 0.1 s^{-1} to100 s^{-1} MRF18L gives the lesser shear stress as compared to the MRF18S and MRF18M1. From this figure it can inferred that MR fluid based on large sized particles (i.e.

MRF18L) provides lesser shear stress compared to MRF18M1 and MRF18S. A sketch of possible chain formation mechanism is illustrated in Fig. 8. As per this figure, spherical shaped small sized particles fill the gap between the flake type large sized iron particles and create a strong iron particle chain enhancing the shear strength of MR fluids.

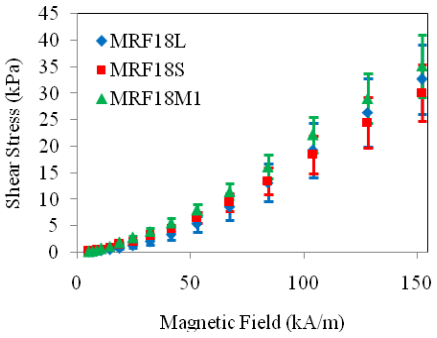

(a) Shear stress of MR fluids

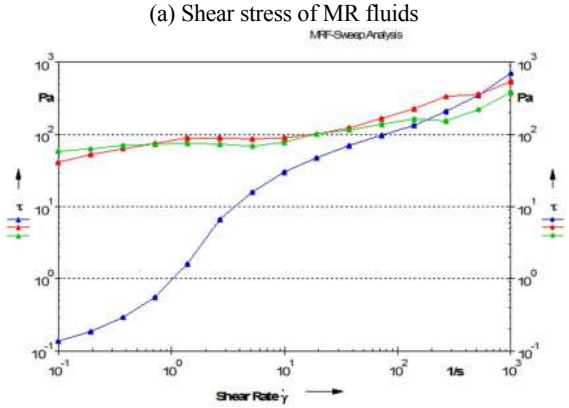

(b) Shear stress flow curve of MR fluids at NO magnetic field

Fig. 7 Shear stress of MR fluid (18% by vol. iron particles) at 10 s^{-1} shear rate and at NO magnetic field

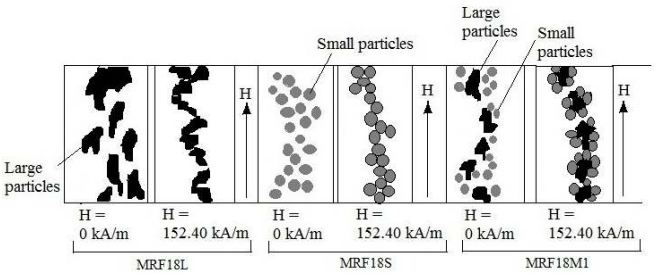

Fig. 8 Chain structure of MR fluids (18% by vol. iron particles)

Fig. 9 (a) shows the shear stress of MR fluid (36% volume fraction iron particle) at 10 s^{-1} shear rate. The shear stress of MRF36M1 increases with increase in the magnetic field and its value is always larger compared to the shear stress of MRF36L and MRF36S. Fig. 9(b) curve shows the shear stress flow curve of MR fluids (36% by vol. of iron particles). The shear stress of MRF36L is lesser as compared to MRF36S and MRF36M1. It is interesting to note from this figure that at higher shear rate, MRF36L is unable to provide higher shear stress particle chains. Fig. 10 illustrates filing of gaps among larger sized flaked shaped particles with smaller sized spherical shaped particles. Due to such action, strong (difficult to shear) particles chains are made and the shear strength of MR fluid increases.

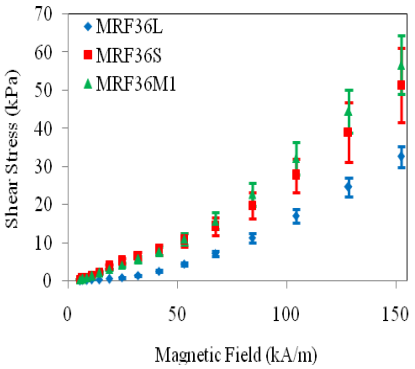

(a) Shear stress of MR fluids at 10 s^{-1} shear

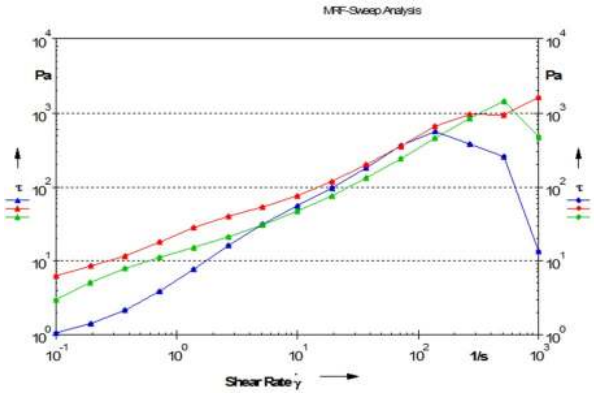

(b) Shear stress flow curve of MR fluids at NO magnetic field

Fig. 9 Shear stress of MR fluid (36 % volume fraction iron particle) at 10 s^{-1} shear rate and at NO magnetic field

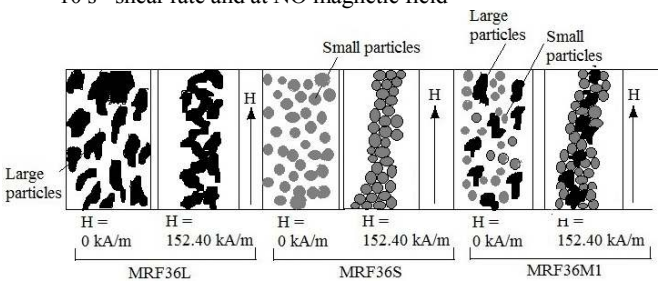

Fig. 10 Chain structure of MR fluids (36% by vol. iron particles)

Fig. 11 (a) shows that shear stress of MR fluids (09% by vol. iron particles) increases with increase in magnetic fields at 100 s^{-1} shear rate. At moderate shear rate, "large sized flake shaped particles" MR fluid with low volume fractions of iron particle shows better performance as compared to the "smaller sized spherical shaped particles" and "mixed sized particles" MR fluids. This is similar observation that was concluded for 10 s^{-1} shear rate. In fig. 11 (b) the shear stress flow curves of MR fluids (09% by vol. of iron particles) at 53.15 kA/m magnetic field have been shown. With increase in shear rate, MRF09L shows higher shear stress as compared to the other MR fluids up to 4 s^{-1} shear rate. At higher shear rates, MRF09M1 fluid performs better than other two fluids. A hypothesis has been illustrated in Fig. 12.

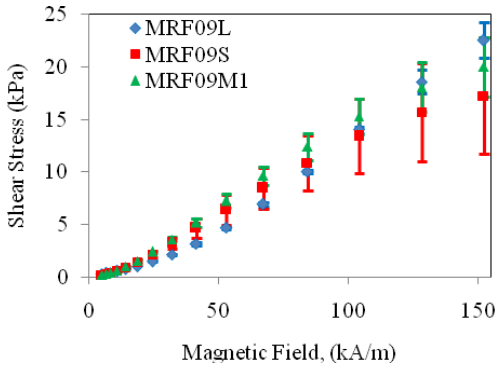

(a) Shear stress of MR fluids at 100 s^{-1} shear rate

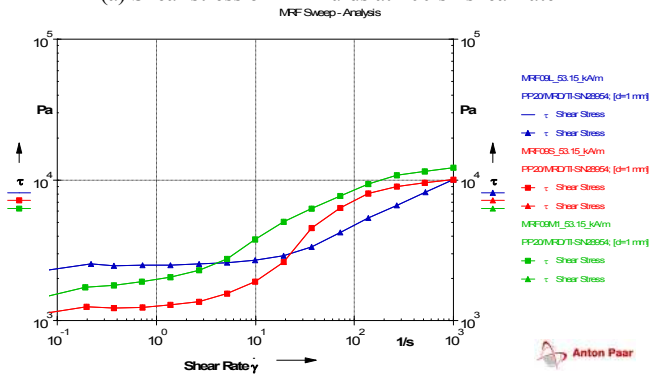

(b) Shear stress flow curve of MR fluids at 53.15 kA/m magnetic field

Fig. 11 Shear stress of MR fluids (09% volume fraction iron particle) at 100 s^{-1} shear rate and at 53.15 kA/m magnetic field

This comparison indicates that particle size, shape and magnetic field affect the shear strength of MR fluid. Higher magnetic field and larger sized particles may provide higher shear strength, provided flake shape of particle is perfectly aligned in the direction of magnetic field.

Fig. 13 (a) shows the shear stress of MR fluids (18% volume fraction iron particle) at 100 s^{-1} shear rate. Fig. 13(b) demonstrates that MRF18L has lesser shear stress compared to MRF18S and MRF18M1 from 0.1 s^{-1} to 5.30 s^{-1} shear rates. MRF18L shows the poor performance as compared to the MRF18M1 and MRF18S, which indicates that with increase in particle percentage and shear rate, the mixed sized particles based MR fluid performs better, which have been detailed in Figure 8 and Fig. 14.

For 18% volume fraction of iron particles, all MR fluids with different sized iron particles complete the chain for constant volume of MR fluids. But in case of mixed sized iron particle based MR fluids, spherical small particles fill the gap between the flake type large sized iron particles which create a strong iron particle chain enhancing the shear strength of MR fluids. However, the shear stress of MRF18M1 and MRF18S are within the statistical error bar. Based on this figure, it can be said that at moderate shear rate MR fluid containing "mixed sized particles" with moderate volume fraction of iron particles shows better performance as compared to shear stress of MR fluids made of moderate volume fractions of "small sized particles" and "large sized particles".

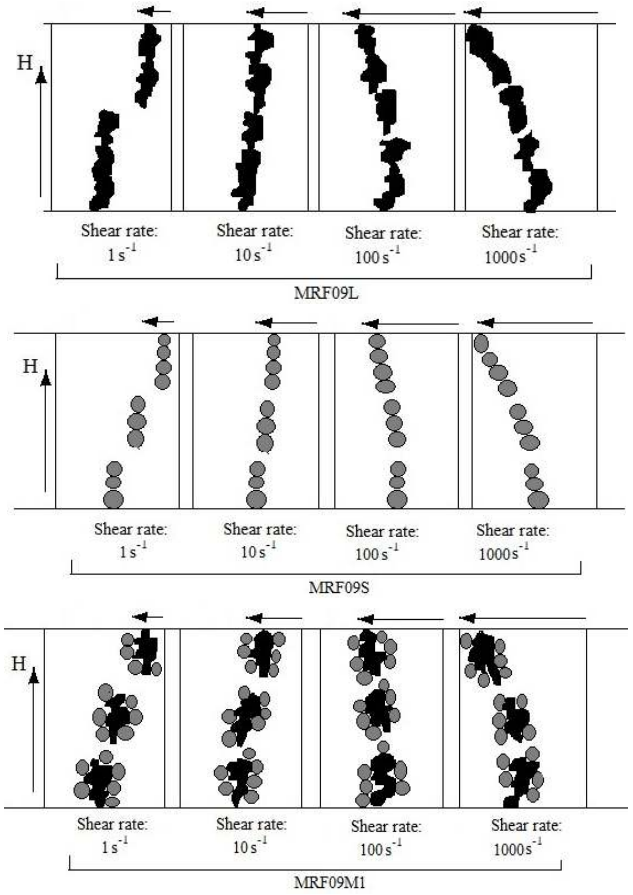

Fig. 12 Chain structures of MR fluids (09% by vol. iron particles) at low and high shear rate for constant magnetic field

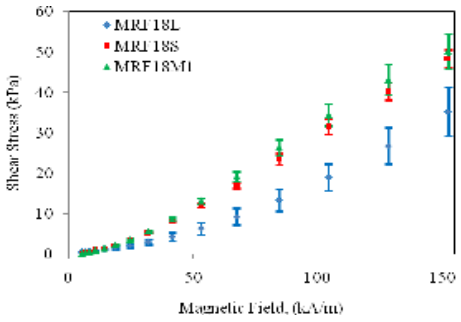

(a) Shear stress of MR fluids at 100 s^{-1} shear rate

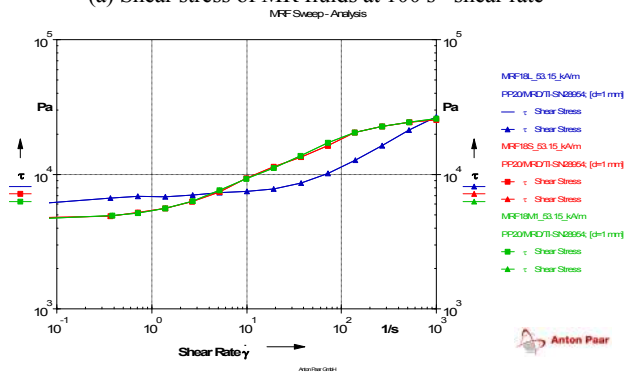

(b) Shear stress flow curve of MR fluids at 53.15 kA/m magnetic field

Fig. 13 Shear stress of MR fluids (18% volume fraction iron particle) at 100 s^{-1} shear rate and at 53.15 kA/m magnetic field

Fig. 15(a) shows the shear stress of MR fluids (36% volume fraction iron particle) at 100 s^{-1} shear rate. The shear stresses of MRF36M1 and MRF36S are almost same and much better in magnitude as compared to that of MRF36L. Fig. 15(b) illustrates that MRF36M1 performs better as compared to the other MR fluids samples at 53.15 kA/m magnetic field. However, shear stress of MRF36L lies in between the shear stress of MRF36S and MRF36M1 from 0.1 s^{-1} to 10 s^{-1} shear rates. MRF36L shows the poor performance as compared to the MRF36M1 and MRF36S, which indicates that with increase in particle percentage and shear rate, the mixed sized particles based MR fluid performs better, which have been detailed in Fig. 10 and Fig. 16.

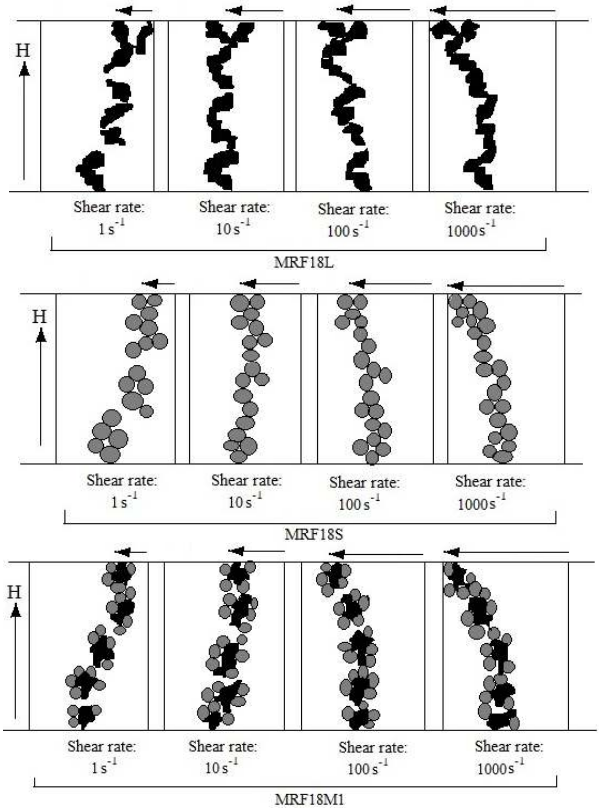

Fig. 14 Chain structure of MR fluids (18% by vol. iron particles) at low and high shear rate for constant magnetic field

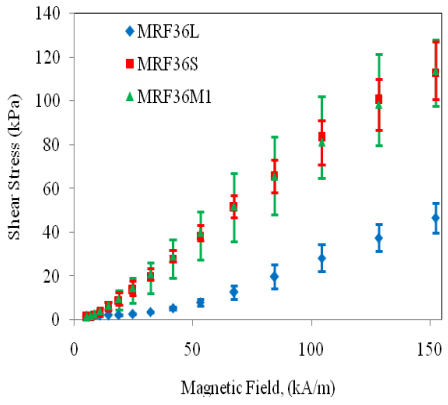

(a) Shear stress of MR fluids at 100 s^{-1} shear rate

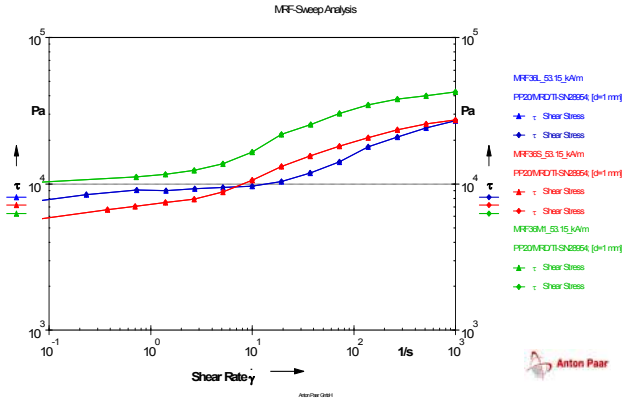

(b) Shear stress flow curve of MR fluids at 53.15 kA/m magnetic field

Fig. 15 Shear stress of MR fluids (36% volume fraction iron particle) at 100 s^{-1} shear rate and at 53.15 kA/m magnetic field

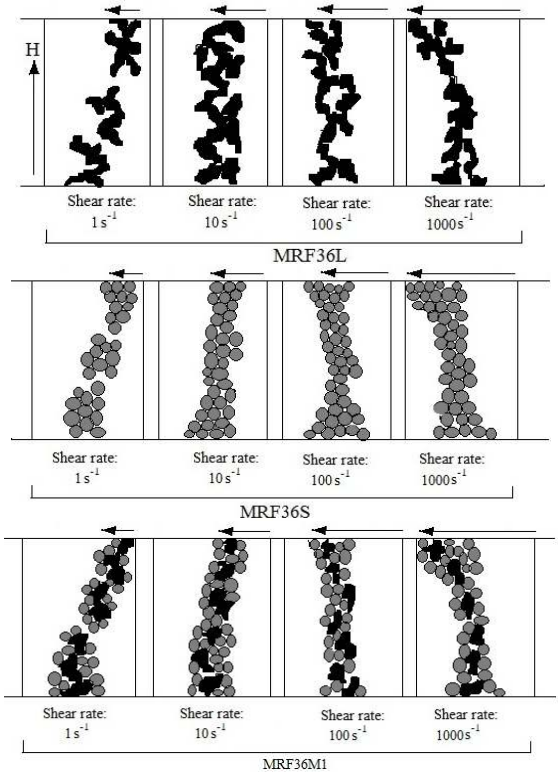

Fig. 16 Chain structure of MR fluids (36% by vol. iron particles) at low and high shear rate for constant magnetic field

Fig. 17 (a) shows the shear stress of MR fluids (09% volume fraction iron particle) at 1000 s^{-1} shear rate. Fig. 17(b) displays that the shear stress of MRF09L is larger compared to the shear stress of MRF09S and MRF09M1 at relatively lower (from 0.1s^{-1} to 138.9 s^{-1}) shear rate. With increase in shear rate MRF09L shows the poor performance as compared to the MRF09M1 and MRF09S. At high shear rate chains formed by flake type iron particles disrupt and decrease in shear stress of MRF09L occurs.

Fig. 18 (a) shows the shear stress of MR fluids (18% volume fraction iron particle) at 1000 s^{-1}. MRF18L shows the poor performance as compared to the MRF18M1 and MRF18S, which indicates that with increase in particle percentage and shear rate, the

mixed sized particles based MR fluid performs better, which have been detailed in Fig. 13 and Fig. 14. Based on this fig., it can be said that at high shear rate MR fluid containing "mixed sized particles" with moderate volume fraction of iron particles shows better performance as compared to shear stress of MR fluids made of moderate volume fractions of "smaller sized spherical shaped particles" and "larger sized flake shaped particles". Fig. 18(b) shows that with increase in shear rate MRF18M1 and MRF18S show similar performances at 152.40 kA/m magnetic field. The shear stress of MRF18L is relatively lesser compared to MRF18S and MRF18M1.

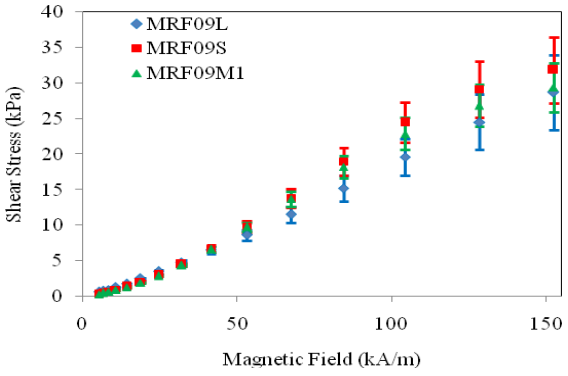

(a) Shear stress of MR fluids at 1000 s^{-1} shear rate

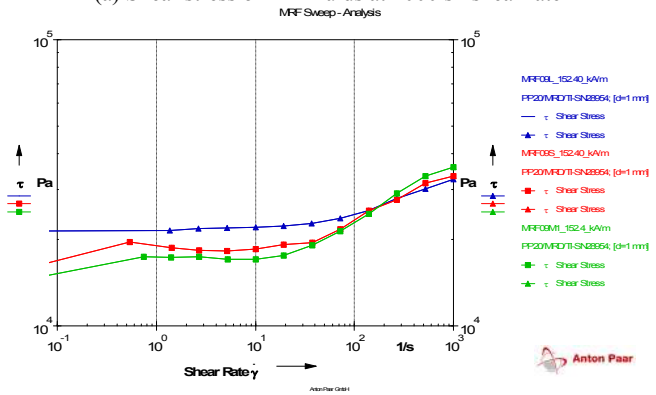

(b) Shear stress flow curve of MR fluids at 152.40 kA/m magnetic field

Fig. 17 Shear stress of MR fluids (09% volume fraction iron particle) at 1000 s^{-1} shear rate and at 152.40 kA/m magnetic fields

Fig. 19 (a) shows the shear stress of MR fluids (36% volume fraction iron particle) at 1000 s^{-1} shear rate. MRF36M1 performs much better in magnitude as compared to that of MRF36S and MRF36L. MRF36L shows the poor performance as compared to the MRF36M1 and MRF36S. This indicates that with increase in particle percentage and shear rate, the mixed sized particles based MR fluid performs better, which have been detailed in Fig. 9 and Fig. 16. The shear stresses of MRF36M1 at 1000 s^{-1} were measured using Modular Compact Rheometer MCR-102 and listed in Table 2. The results of this table indicate that there is a limitation on motor of Rheometer MCR-102. The shear rate decreases as magnetic field increases from104.30 kA/m to 152.40 kA/m. Hence, shear stress at 104.30 kA/m, 128.40 kA/m and 152.40 kA/m magnetic field, is same i.e. 128.3 kPa as shown in Table 2. Fig. 19 (b) demonstrates the shear stress flow curve of MR fluids (36% by vol. iron particles) at 152.40 kA/m magnetic fields. Very different behaviour of MRF36M1 and MRF36S is observed in the Fig. 19(b). At 152.40 kA/m magnetic field, achieving high shear rate (greater than 120.6 s^{-1} for MRF36S and more than 24.02 s^{-1} for MRF36M1) is not possible on the Anton Paar Rheometer (MCR-102).

Table 2 Shear stress measurement of MRF36M1 at various input currents at 1000 s^{-1} shear rate

Magnetic. Field	Shear Rate_ trial1	Shear Stress_ trial1	Shear Rate_ trial2	Shear Stress_trail2
[A/m]	[s^{-1}]	[Pa]	[s^{-1}]	[Pa]
5,326	1,000	1,715	1,000	2,274
6,753	1,000	2,296	1,000	2,468
8,487	1,000	2,795	1,000	2,985
10,800	1,000	3,852	1,000	3,891
14,320	1,000	5,397	1,000	5,087
18,850	1,000	7,905	1,000	7,179
24,710	1,000	10,460	1,000	9,892
32,170	1,000	15,250	1,000	13,580
41,570	1,000	21,220	999.6	19,740
53,140	999.9	31,210	1,000	30,980
67,420	999	59,120	999.4	49,500
84,440	999.8	98,810	998.7	99,530
1,04,300	462.1	1,28,300	270.3	1,28,300
1,28,400	197.4	1,28,300	123.9	1,28,300
1,52,400	118.9	1,28,300	57.44	1,28,300

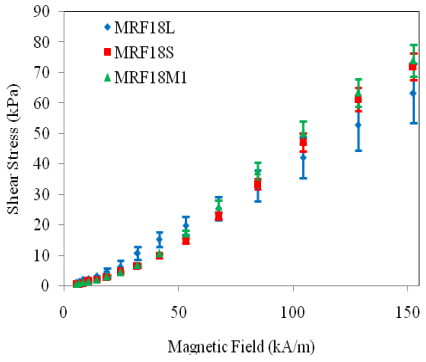

(a) Shear stress of MR fluids at 1000 s^{-1} shear rate

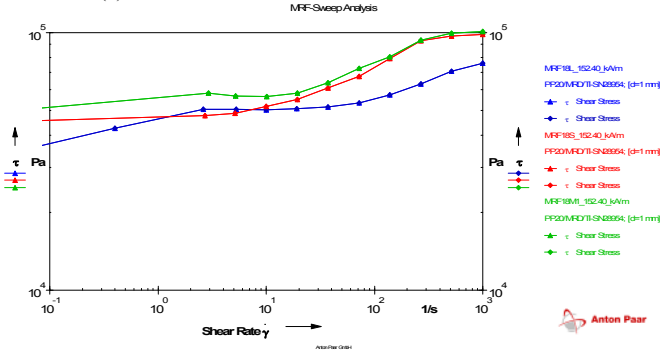

(b) Shear stress flow curve of MR fluids at 152.40 kA/m magnetic field

Fig. 18 Shear stress of MR fluids (18% volume fraction iron particle) at 1000 s^{-1} shear rate and at 152.40 kA/m magnetic fields

It can be interpreted that with increase in volume fraction of iron particles, the shear stress of MR fluids with "mixed sized particles" show better performance compared to the MR fluids containing "smaller sized spherical shaped particles" and "larger sized flake shaped particles" at higher shear rate. The "larger sized flaked shaped particles" MR fluid with low volume fractions iron particles is a good option at low to moderate shear rate. The iron particle chains of "larger sized flake shaped particles" MR fluids with low volume fraction breaks at high shear rate due to their flake type structure. In brake application, where two rotating bodies are moving relative to each other, sedimentation is not a problem. This has been described by Sarkar and Hirani [17]. Hence larger sized particles may be permitted.

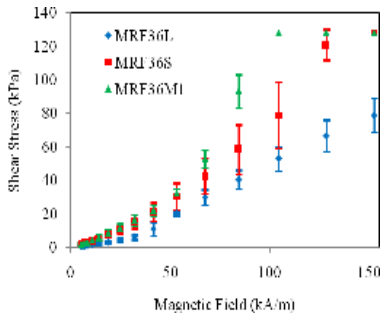

(a) Shear stress of MR fluids at 1000 s^{-1} shear rate

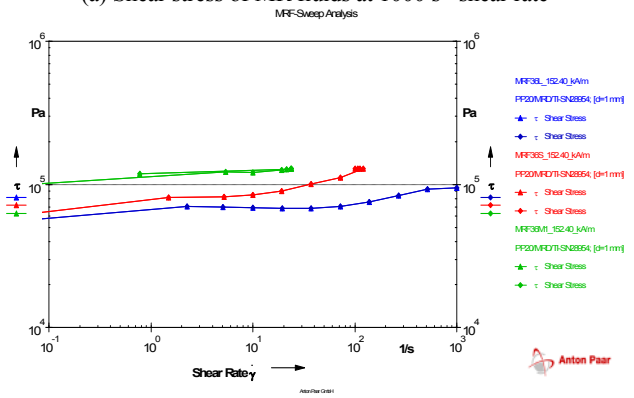

(b) Shear stress flow curve of MR fluids at 152.40 kA/m magnetic field

Fig. 19 Shear stress of MR fluids (36 % volume fraction iron particle) at 1000 s^{-1} shear rate

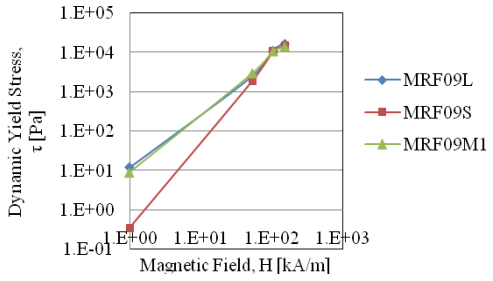

(a) Comparison of dynamic yield stress of MR fluids (09% volume fractions of iron particles)

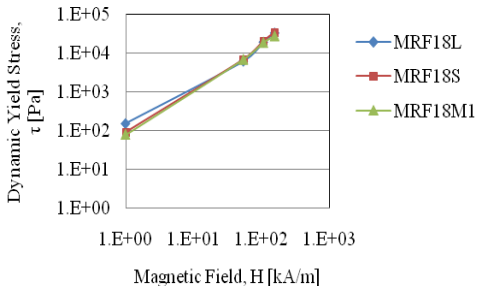

(b) Comparison of dynamic yield stress of MR fluids (18% volume fractions of iron particles)

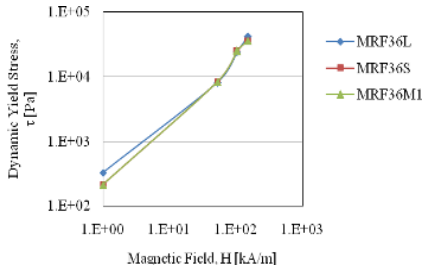

(C) Comparison of dynamic yield stress of MR fluids (18% volume fractions of iron particles)

Fig. 20 Dynamic yield stress vs. magnetic field strengths for MR fluids

To understand the magnetic field dependence on shear stress, the data (stress of MRF09L, MRF09S, MRF09M1; MRF18L, MRF18S, MRF18M1; and MRF36L, MRF36S, MRF36M1) at zero shear rate for various magnetic fields have been plotted (shown in Fig. 20) in log-log scale. The results have been compared with those provided by Fang et al. [15, 18] and Hato et al. [16].

4. Conclusion

The particle size distributions were measured using HORIBA Laser scattering Particle Size Distribution Analyzer LA-950. The following observations have been made from the analysis.

- The mean size and standard deviation of the "smaller sized spherical shaped particles" distributions are 9.27 μm and 4.63 μm respectively.
- The mean size and standard deviation of the "large sized particle" distributions are 120.85 μm and 56.05 μm respectively.
- The "small sized particles" are spherical in shape and the "larger sized particles" are of flake shape. To explore the effect of particle sizes, nine MR fluids containing small, large and mixed sized carbonyl iron particles with three concentrations (9%, 18% and 36% by volume) have been synthesized. The shear stresses of these MRF samples have been measured using ANTON PAAR MCR-102 Rheometer. The following observations have been made from the experimental data.
- The "larger sized flake shaped particles" MR fluids with low volume fraction iron particles perform better at low shear rate. At low shear rate (10 s^{-1}), all three types of MR fluids show

increase in shear stress with increase in particle volume percentage.

- At moderate shear rate MR fluid made of "large sized particles" performs better only at low volume fractions iron particles compared to MR fluids made of low volume fraction "small sized particles" and "mixed sized particles". At moderate volume fraction "mixed sized particle" MR fluids provide the best performance among all three.
- With increase in volume fraction of iron particles, the shear stress of MR fluids with "mixed sized particles" show better performance compared to the MR fluids containing "small sized particles" and "large sized particles" at higher shear rate.

REFERENCES

[1] J. D. Carlson, "What makes a good MR fluid?" *Journal of Intelligent Material Systems and Structures*, **13**, 431-435 (2002) DOI: 10.1106/104538902028221

[2] S. Donga, K. Q Lua, J. Q. Suna, and K. Rudolphb, "Rehabilitation device with variable resistance and intelligent control" *Medical Engineering & Physics*, **27**, 249-255 (2005) DOI: 10.1016/j.medengphy.2005.06.005

[3] A. Spaggiari and E. Dragoni, "Effect of pressure on the flow properties of magnetorheological fluids" *Journal of Fluids Engineering*, **134**, 091103 (2012) DOI: 10.1115/1.4007257

[4] E. Lemaire, A. Meunier, G. Bossis, J. Liu, D. Felt, P. Bashtovoi, and N. Matoussevitch, "Influence of the particle size on the rheology of magnetorheological fluids" *Journal of Rhelogy*, **39**, 1011-1020 (1995) DOI: 10.1122/1.550614

[5] D. Kittipoomwong, D. J. Klingenberg, and J. C. Ulicny, "Dynamic yield stress enhancement in bidisperse magnetorheological fluids" *Journal of Rhelogy*, **49**, 1521-1538 (2005) DOI: 10.1122/1.2085175

[6] H. Chiriac and G. Stoian, "Influence of particle size distributions on magnetorheological fluid performances" *Journal of Physics: Conference Series*, **200**, 072095 (2010) DOI: 10.1088/1742-6596/200/7/072095

[7] B. J. Jung, Y. U. Seong, H. R. Jee, and D. S. Kyung, "Synthesis and characterization of mono disperse magnetic composite particles for magnetorheological fluid materials" *Colloids and Surfaces A: Physicochemical and Engineering Aspects*, **260**, 157-164 (2005) DOI: 10.1016/j.colsurfa.2005.03.020

[8] N. M. Wereley, A. Chaudhuri, J. H. Yoo, J. H. John, S. Kotha, A. Suggs, R. Radhakrishnan, B. J. Love, and T. S. Sudarshan, "Bidisperse magnetorheological fluids using Fe particles at nanometer and micron scale" *Journal of Intelligent Material Systems and Structures*, **17**, 393-401 (2006) DOI: 10.1177/1045389X06056953

[9] M. T. López-López, P. Kuzhir, A. Meunier and G. Bossis, "Synthesis and magnetorheology of suspensions of submicron sized cobalt particles with tunable particle size" *Journal of Physics: Condensed Matter*, **22**, 324106 (2010) DOI: 10.1088/0953-8984/22/32/324106

[10] Sigma Aldrich Product. Available at: http://www.sigmaaldrich.com/catalog/product/aldrich/12310, (accessed on March 07, 2015) http://www.sigmaaldrich.com/catalog/product/aldrich/44890, (accessed on March 07, 2015)

[11] "Lord Corporation Products," http://www.lord.com, accessed on June 20 (2014)

[12] J. D. G. Duran, G. R. Iglesias, A. V. Delgado, L. F. Ruiz-Moron, J. Insa, and F. Gonzalez-Caballero, "Stability and flow behavior of a magnetorheological lubricant in a magnetic shock absorber" *Tribology Transactions*, **51**, 271-277 (2008) DOI: 10.1080/10402000701793963

[13] W. L. Song, S. B. Choi, J. Y. Choi, and C. H. Lee, "Wear and friction characteristics of magnetorheological fluid under magnetic field activation" *Tribology Transactions*, **54**, 616-624 (2011) DOI: 10.1080/10402004.2011.584365

[14] J. Seok J, S. Lee, K. Jang, B. K. Min, and S. J. Lee, "Tribological properties of a magnetorheological (MR) fluid in a finishing process" *Tribology Transactions*, **52**, 460-469 (2009) DOI:10.1080/10402000802687932

[15] F. F. Fang, H. J. Choi, and M. S. Jhon, "Magnetorheology of soft magnetic carbonyl iron suspension with single-walled carbon nano tube additive and its yield stress scaling function" *Colloids and Surfaces A Physicochemical and Engineering Aspects*, **351**, 46-51 (2009) DOI: 10.1016/j.colsurfa.2009.09.032

[16] M. H. Hato, H. J. Choi, H. H. Sim, B. O. Park, and S. S. Ray, "Magnetic carbonyl iron suspension with organo clay additive and its magnetorheological properties" *Colloids and Surfaces A Physicochemical and Engineering Aspects*, **377**, 103-109 (2011) DOI: 10.1016/j.colsurfa.2010.12.029

[17] C. Sarkar and H. Hirani, "Theoretical and experimental studies on magnetorheological brake operating under compression plus shear mode" *Smart Materials and Structures*, **22**, 115032 (2013) DOI: 10.1088/0964-1726/22/11/115032

[18] F. F. Fang, Y. D. Liu, H. J. Choi, and Y. Seo, "Core shell structured carbonyl iron microspheres prepared via dual-step functionality coatings and their magnetorheological response" *ACS Applied Materials & Interfaces*, **3**, 3487-3495 (2011) DOI: 10.1021/am200714p